Spectroscopic and Optimization Modeling Study of Nitrous Acid in Aqueous Solution

Eoin Riordan, Nicholas Minogue, David Healy, Paul O'Driscoll, and John R. Sodeau*

Department of Chemistry, University College Cork, Ireland

Received: March 31, 2004; In Final Form: September 21, 2004

Nitrous acid (HONO) and the nitrite ion represent a particularly important conjugate pair of trace species with regard to heterogeneous behavior within the bulk, and on the surface, of aqueous atmospheric dispersions: this role results from their chemical reactivity, photolysis pathways, solubility, and ambient concentration levels. The actual ratio of NO_2^-: HONO in solution is determined by the pH and the nitrous acid dissociation constant (pK_a) which is generally quoted in the literature as 3.27 at 298 K. However there is much disagreement in published works as to the exact value, which should be used in model calculations relevant to the atmosphere. Furthermore even though the nitrite ion is known to absorb solar radiation in the 300−400 nm region and represents a dominant source of •OH radicals in surface seawater, large variations in the measured molar decadic absorption coefficients, ϵ, for nitrite ions (and aqueous HONO) are evident in the literature. In the current study, using a UV−vis spectrometric approach with careful baseline subtraction, the relevant ϵ values for the nitrite ion were determined to be 8.16 ± 0.08 M^{-1} cm^{-1} for the $n\pi^*$ transitions at 290 nm and 22.1 ± 0.22 M^{-1} cm^{-1} at 354 nm. For HONO, the wavelength maximum for the strongest vibronic band in solution was found at 372 nm with an ϵ value of 60.52 ± 0.6 M^{-1} cm^{-1}. Using the Henderson−Hasselbalch equation and the above data, a value of 2.8 ± 0.1 is therefore reported here for the pK_a of nitrous acid. A Newton-Gauss method was then employed to solve a set of nonlinear equations defining the chemical speciation model for HONO in solution using an algorithm written in FORTRAN 90. A model based on a simple one-step protonation worked well for intermediate pHs (6−3) but departed from the experimental observations in highly acidic media. A two-step equilibrium model involving the nitroacidium ion, H_2ONO^+, gave a much closer fit in the very acidic region, while having little or no effect on the pH 6−3 section of the profile.

Introduction

Aqueous dispersions of particles play a major role in atmospheric chemistry because a number of their physicochemical features are of direct relevance to our understanding of compositional change in the troposphere. These include solubility measurements, the nature of the gas/liquid/solid interface, and the precise relationship between gas-phase components and their dissolved counterparts in aqueous aerosols. For these reasons, laboratory studies of the kinetics, thermodynamics, and accommodation of a variety of heterogeneous systems relevant to the atmosphere have become increasingly sophisticated and accurate over the past decade. One of their central roles is in determining the contribution of so-called "missing" chemical intermediates and pathways for trace species in computational models of the atmosphere.

Predictive understanding of the reactive pathways available within the bulk and on the surface of atmospheric dispersions has been little studied because our knowledge of heterogeneous transformations currently relies on a database comprised of measurements made for few chemicals on a limited number of interfaces. Nitrous acid (HONO) and the nitrite ion represent a particularly important conjugate pair of trace species in this regard due to their reactivity,[1,2] solubility and ambient levels in the atmosphere.[3,4]

$$HONO + H_2O \rightleftharpoons H_3O^+ + NO_2^- \quad (1)$$

The environmental sources of nitrite ions in solution are not fully understood. Certainly, they are a product of the oxidation of nitrogen-containing organic matter, and therefore, their presence in water is very often an indication of recent microbial contamination.[1] Also, dissolved nitrogen dioxide gas produces NO_2^- as indicated in reactions 2 and 3 below

$$NO_{(aq)} + NO_{2(aq)} + H_2O \rightarrow 2NO_2^- + 2H^+ \quad (2)$$

$$2NO_{2(aq)} + H_2O \rightarrow NO_2^- + NO_3^- + 2H^+ \quad (3)$$

The rate coefficients of reactions 2 and 3 have been measured to be 3×10^8 M^{-1} s^{-1} and 1×10^8 M^{-1} s^{-1}, respectively.[5] They clearly proceed far too slowly to contribute to the removal of gas-phase nitrogen oxides or to lead to an increase in cloudwater acidification.[6] Hence under ambient conditions, aqueous nitrite ions have been detected in both cloud and fog droplets at concentrations below 1 nM.[1]

In sulfur-polluted urban environments, aqueous nitrite concentrations of up to several hundred μM have been observed.[6] This phenomenon has been attributed in part to reaction 4 shown below

$$2NO_{2(aq)} + HSO_3^- + H_2O \rightarrow 2NO_2^- + 3H^+ + SO_4^{2-} \quad (4)$$

Another source of nitrite ions is gas-to-liquid transfer of gaseous nitrous acid. HONO concentrations in the atmosphere vary diurnally, as a result of daytime photolysis ($\lambda < 400$ nm) to NO and the hydroxyl radical, reaching maximum night-time

* To whom correspondence should be addressed.

10.1021/jp040269v CCC: $30.25
Published on Web 01/20/2005

values, which range from 0.5 ppbv in rural areas to 10 ppbv in polluted urban environments. It has a variety of homogeneous, heterogeneous, and direct injection sources and a moderately high Henry's law constant compared to other trace gases.[7] Hence N(III) solution concentrations are highly susceptible to its level in the atmosphere. The importance of this source is governed by the acidity of the water because at pH = 3 and at a mixing ratio of 1 ppbV of HONO, N(III) eventual solution concentrations will be less than 0.1 μmol dm^{-3}. On the other hand, a pH of 6 increases the N(III) concentration to 15 μmol dm^{-3}. The actual ratio of NO_2^-:HONO in solution is determined by the pH and the nitrous acid dissociation constant (K_a) which is generally quoted in the literature as 5.1×10^{-4} M at 298 K ($pK_a = -\log K_a = 3.27$).

The nitrite ion absorbs solar radiation in the 300−400 nm region and can also be photolyzed to eventually form the hydroxyl radical. This particular pathway is known to be a dominant source of •OH in surface seawater[8,9] and is also important in dew waters.[10,11] However, large variations in the molar absorption coefficients for nitrite ions (and aqueous HONO) are evident in the literature.

The hydroxyl radical, of course, represents one of the atmosphere's most reactive compounds and determines the lifetime of many species in the troposphere. Therefore, given the above remarks, it is clearly important to incorporate an agreed value for the nitrous acid dissociation constant (K_a) into relevant atmospheric models. Furthermore, since both nitrite ions and HONO in solution can be photolyzed to produce hydroxyl radicals, a precise knowledge of the molar absorption coefficients of the acid and its conjugate species is also required for inclusion in tropospheric models.

The whole range of environmental matrixes that can be termed "atmospheric waters" actually range in pH from 1.95 to 7.74,[12−14] and therefore, the chemical behavior of HONO in highly acidic solution may be relevant to heterogeneous tropospheric chemistry. It has been suggested that the nitrosonium ion, NO^+, exists at pH $\leq$ 1 and that weakly bound complexes of NO^+ with water, or even the nitrous acidium ion (H_2ONO^+), exist below pH = 2.2 [15,16] as follows:

$$HONO \overset{H^+}{\rightleftharpoons} H_2ONO^+ \rightleftharpoons NO^+ + H_2O \qquad (5)$$

In synthetic chemistry, kinetic studies have shown that several nitrosation reactions carried out using HONO in highly acidic solution proceed via formation of H_2ONO^+, which acts as the nitrosating agent.[17−19] Hence a number of ab initio calculations on the nitrous acidium ion have been performed.[20,21] For example, Nguyen and Hegarty used theoretical methods to determine the most likely protonation site on HONO.[16] Of the two oxygen atoms, protonation at the central oxygen was found to produce a more stable isomer than at the terminal oxygen. In a more recent study, Francisco corroborated the earlier findings and also calculated the vibrational frequencies of the different isomers of the H_2ONO^+ ion.[22]

The general aim of the current study was to explore the role of acidity in atmospheric water, which is central to understanding both reactive uptake at the interface and reaction mechanisms within, say, an aerosol droplet. To achieve this aim, it is important that reliable data on fundamental values such as the dissociation constant for nitrous acid is known with some precision. The main target of the computational work performed for very low pH solution values was to determine any potential involvement of the nitrous acidium ion, H_2ONO^+, in heterogeneous processing relevant to the troposphere.

The methodology employed is based on a complementary UV−vis spectroscopic and an optimization computer modeling study of the HONO/NO_2^- conjugate pair in order to address many of the issues discussed above. Hence a precise value of the acid-dissociation constant of nitrous acid (K_a) has been obtained using two independent methods and the results compared with the available literature data. Furthermore the spectra were used to reevaluate the molar absorption coefficients of the two species within the UV−vis region. Finally, a computer program, written in Fortran 90, was applied to the equilibrium systems represented both by reaction 1 and the two-step process summarized by reaction 5 in order to model the aqueous speciation.

Experimental and Computational Methodologies

Spectroscopic Measurements and Quantitative Determination of Aqueous Species. UV−vis absorbance spectra were recorded with a Hewlett-Packard 8453 diode-array spectrophotometer. This is a single-beam instrument capable of acquiring spectra from 190 to 800 nm at a resolution of 1 nm and utilizes two light sources: a deuterium arc lamp in the UV range (consistent in the 190−380 nm region) and a tungsten−halogen lamp in the visible spectrum (consistent in the 380−800 nm region). The absorbance measurement errors associated with such a spectrometer are <0.005.

The pH values of the aqueous solutions were measured to within ±0.1 of a pH unit using a Pasco ScienceWorkshop pH Sensor, which consists of a gel-filled Ag−AgCl electrode.

Optimization Modeling of Aqueous Ionic Solutions. Aqueous ionic solutions can be described by Debye−Hückel theory, which accounts for a full system development from a random distribution of charges in highly dilute solutions through to a pattern of alternating positive and negative charges at slightly higher concentrations.[23] The basis for Debye−Hückel theory is founded in the long range Coulombic interactions between charge carriers. In a dilute aqueous solution, the time-averaged distribution of solute species displays the existence of arrangements of ions of the like charge polarity around an oppositely charged central ion. It is assumed that the individual ion activity coefficients are not dependent on the properties of each ion and can be described by the mean ion activity coefficient, $\gamma_\pm$

$$\ln \gamma_\pm = -A_x\left[\frac{\sqrt{I}}{1+1.2\sqrt{I}} + \frac{2}{1.2}\ln(1+1.2\sqrt{I})\right] \qquad (6)$$

where A_X is the Debye−Huckel parameter

$$A_x = (1/3)(2\pi N_A d_l/M_l)^{1/2}(e^2/4\pi\epsilon_0 D_k T)^{3/2} \qquad (7)$$

In dilute aqueous solution, the time-averaged distribution of solute species can be formulated on the basis of arrangements of ions with like charge polarity clustering around an oppositely charged central ion. This overall distribution is termed the "ionic atmosphere" of the central ion. Electrostatic interaction between the central ion and its ionic atmosphere leads to a lowering in the energy which can be identified with the deviation of Gibbs free energy from that of an ideal solution. As described by Debye and Hückel, this description leads to a low concentration "limiting law" in which the basic variable is ionic strength, I, defined as

$$I = \frac{1}{2}\sum_i z_i^2 m_i \qquad (8)$$

(m_i and z_i are the molalities and charges of all ionic species in solution).

Optimization techniques are widely used in fields of engineering and design, though they have been infrequently applied to chemical systems. In essence, they use well-established numerical methods to solve a set of equations that describe a system. These methods of analysis are usually iterative and subsequently require the use of computational techniques. A Newton-Gauss method was employed in this study to solve a set of nonlinear equations defining the chemical speciation model for HONO in solution using an algorithm written in FORTRAN 90.

The first model considered only the simple protonation step, nitrite ion to nitrous acid.

Therefore, four variables were includeded: [HONO], $[NO_2^-]$, $[H^+]$, and $[OH^-]$. Four equations were solved in the model to evaluate these quantities using the experimentally determined nitrous acid dissociation constant (K_a) and the ionic product of water (K_w) as the limiting parameters. The equations consist of a mass balance of N(III)

$$\mathrm{N(III)} - [\mathrm{NO_2^-}]_{aq} - [\mathrm{HONO}]_{aq} = 0 \qquad (9)$$

a charge balance

$$[\mathrm{H}]_{aq}^{+} + [\mathrm{Na}]_{aq}^{+} - [\mathrm{OH}]_{aq}^{-} - [\mathrm{NO_2^-}]_{aq} - [\mathrm{Cl^-}]_{aq} = 0 \qquad (10)$$

the dissociation of water

$$K_w - [\mathrm{OH^-}]_{aq}\,[\mathrm{H^+}]_{aq}\,\gamma_{\pm}^{\,2} = 0 \qquad (11)$$

and the dissociation of nitrous acid

$$K_a\,[\mathrm{HONO}]_{aq} - [\mathrm{NO_2^-}]_{aq}[\mathrm{H^+}]_{aq}\,\gamma_{\pm}^{\,2} = 0 \qquad (12)$$

where $\gamma_{\pm}$ is the mean ionic activity coefficient. The N(III) concentration is the input variable and the program calculates the pH of the system for a range of added HCl concentrations. The results can then be displayed in the form of a graph of pH vs acid added.

This model was then modified to consider the possible second protonation step, nitrous acid to nitrous acidium ion. The introduction of the H_2ONO^+ ion simply increases the number of variables from four to five, whereas a second equilibrium step leads to a second acid dissociation constant (K_{a1}) being introduced. The mass balance of N(III) then becomes

$$\mathrm{N(III)} - [\mathrm{NO_2^-}]_{aq} - [\mathrm{HONO}]_{aq} - [\mathrm{H_2ONO^+}]_{aq} = 0 \qquad (13)$$

and the charge balance is similarly altered

$$[\mathrm{H}]_{aq}^{+} + [\mathrm{Na}]_{aq}^{+} + [\mathrm{H_2ONO^+}]_{aq} - [\mathrm{OH}]_{aq}^{-} - [\mathrm{NO_2^-}]_{aq} - [\mathrm{Cl^-}]_{aq} = 0 \qquad (14)$$

The dissociation of water and the dissociation of nitrous acid remain unchanged but a fifth equation must be introduced to describe the new equilibrium

$$K_{a1}\,[\mathrm{H_2ONO^+}]_{aq} - [\mathrm{HONO}]_{aq}[\mathrm{H^+}]_{aq} = 0 \qquad (15)$$

A variety of plots result from the treatment and include graphical representations of the mole fraction of HONO vs pH for comparison between model and experimental results.

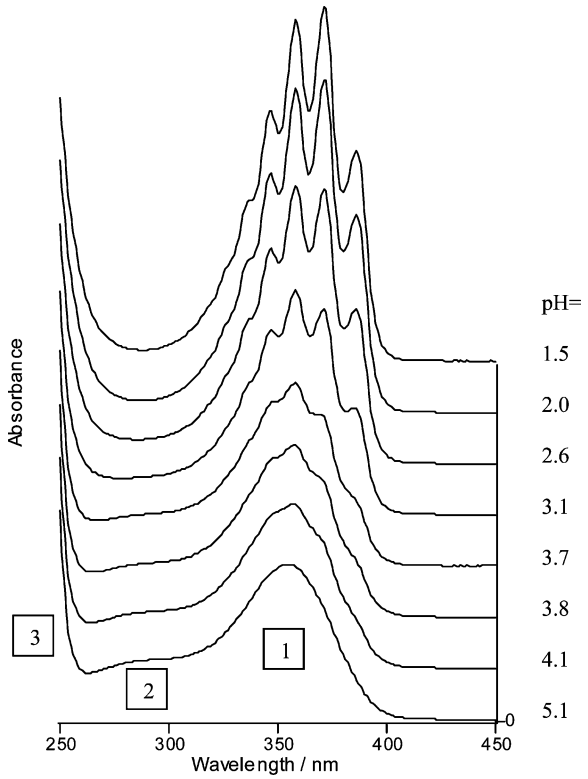

Figure 1. UV−visible spectra of 0.03M $NaNO_2$ and HCl solutions (at various pH values).

Results and Discussion

Electronic Absorption Spectra of Aqueous Nitrite Ions and Nitrous Acid. UV−vis spectra of $NaNO_2$ dissolved in aqueous solution (concentration range, 0.02−0.06 M) were recorded. The nitrite ion displays three distinct regions of absorption: two weak, broad bands with maxima at 354 and 290 nm and one very strong band with a maximum below 250 nm. These bands are labeled 1, 2, and 3 in Figure 1. It was not possible to determine the λ_{max} of the shortest wavelength band in the current experiments because the spectrometer was not flushed with nitrogen gas. However, Strickler and Kasha previously have recorded aqueous NO_2^- spectra under appropriate conditions and assign a wavelength maximum of 210 nm for this feature.[24]

The general consensus in the literature reports is that the weaker bands can be classified as $n \rightarrow \pi^*$, whereas the strong peak is $\pi \rightarrow \pi^*$ in nature.[24−27] However the $n_{Nitrogen}$ or n_{Oxygen} identities of the parent nonbonding orbital (n) for the weak bands have been a matter of dispute.[28] Furthermore, some studies have classified the 210 nm absorption as an electron-transfer transition between the ion and the solvent rather than $\pi \rightarrow \pi^*$.[24]

The pH values of the above nitrite ion solutions were adjusted from 6 to 1.5 using both H_2SO_4 and HCl (in separate experiments). Above pH 5, the solutions contain mostly (>99%) nitrite ion. The addition of acid affects the (NIII) speciation by converting NO_2^- to $HONO_{(aq)}$ as shown in eq 16

$$\mathrm{NO_2^-} + \mathrm{H_3O^+} \rightleftharpoons \mathrm{HONO} + \mathrm{H_2O} \qquad (16)$$

This is clearly evidenced in the spectra displayed in Figure 1 by an observed decrease in the $n \rightarrow \pi^*$ absorption centered at 290 nm. It is also of note that the broad band at 354 nm becomes more structured as acidity increases.

TABLE 1: Aqueous HONO Vibronic Structure in 300−400 nm Region

λ	cm^{-1}	cm^{-1} gap	error
387	25840		
372	26882	1042	139
358	27933	1051	150
346	28902	969	162
335	29851	949	173
326	30675	824	183
317	31546	871	194
309	32363	817	204
301	33223	860	215
292	34247	1024	228

Adopting the literature value for HONO of a pK_a = 3.27,[29] then at pH = 1.5 the 0.03M solution shown in Figure 1 would be expected to contain <1% NO_2^- ion. Therefore, this low-pH mixture can be regarded as a baseline sample of aqueous nitrous acid. Nine distinguishable features can be identified in aqueous solution[30] within the ca. 300−400 nm region and their positions are summarized in Table 1. Their origin is associated with hydrogen-bonded mixtures of the cis and trans isomers, which exist in the gas-phase.

An error of ±1 nm (as a result of instrumental limitations) is associated with each peak but the resultant spectra clearly indicate a progression associated with the N−O stretching mode of electronically excited HONO, as previously discussed.[31−33]

Quantitation of the Nitrite Ion and Nitrous Acid Components from the UV−vis Spectra. The molar absorption coefficients (ϵ) of aqueous nitrite ions in the range 270−400 nm were evaluated for the series of NO_2^- concentrations outlined above at pH = 5.

Figure 2 shows a plot of absorbance vs concentration at 290 and 354 nm. Clearly, Beer's law is obeyed over the concentration range 0.02−0.06 M. The plot gives values of 8.16 and 22.10 M^{-1} cm^{-1} for the molar absorption coefficients at 290 and 354 nm respectively. A maximum error of 1% is associated with the ϵ values.

Table 2 provides a comparison between the available literature data for the relevant molar absorption coefficients and the current study. Agreement between the four studies appears very close although when error estimates are included, there is, for example, a possible 10% deviation between the current study and that of Wetters. Clearly, more data sets need to be acquired in order to establish the ϵ values with more precision.

As discussed above, the nitrous acid spectrum consists of several vibronic features in the 300−400 nm region which become increasingly prominent as pH is reduced below 5.

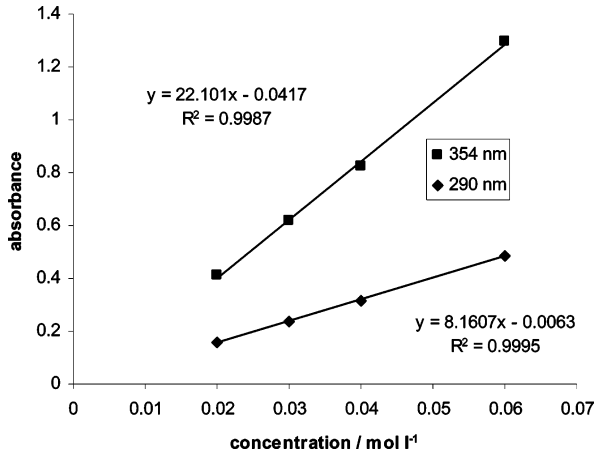

Figure 2. Plot of absorbance vs concentration for nitrite ion solutions and evaluation of ϵ.

TABLE 2: Comparison of ϵ Values for the Aqueous Nitrite Ion n → π^* Transitions

ϵ/M^{-1} cm^{-1}		
290 nm	354 nm	ref
8.84 ± 0.06	22.93 ± 0.16	Zuo[2]
	22.8 ± 0.09	Fischer[34]
	23.3 ± 0.8	Wetters[38]
8.16 ± 0.08	22.1 ± 0.22	current study

However, to fully quantify these absorptions, it is clearly necessary to remove the contribution of NO_2^- from the spectra. Arakaki et al. have lowered the pH of a series of nitrite ion solutions to 1.1 by adding sulfuric acid;[13] such solutions contain >99% HONO at this pH. A simple calibration plot (as in the case of nitrite ion) then yields the molar absorption coefficient data as long as the simple nitrite ion/nitrous acid equilibrium shown in reaction 1 is actually maintained. If a second equilibrium step becomes necessary to fully explain the chemistry at low pH (<2), as discussed above, an overestimation of the concentration of nitrous acid in solution would result.

In the current study, a more rigorous quantitative method than that employed by Arakaki was developed. A NO_2^- reference spectrum was obtained by adding base (NaOH) to a 0.02 M NO_2^- solution to reach pH = 10 value. The resultant spectrum was subtracted from each of the N(III) solution spectra with the 290−300 nm region set as baseline because HONO has no absorbance between these limits. Such a procedure removes the NO_2^- contributions from the spectra and leaves only those belonging to HONO.

Hence molar absorption coefficients over the entire wavelength range can be evaluated for nitrous acid simply by plotting absorbance vs [HONO]. This method simply assumes [HONO] is equal to [N(III)] − [NO_2^-] in the pH region 6−3 and is not subject to the speciation problems discussed above.

Using the above Beer's law procedures, ϵ values for HONO and NO_2^- can be calculated from the spectra over the full range 270−400 nm, and these data are displayed in Table 3. The maximum molar absorption coefficient for HONO was found at 372 nm, which is in close agreement with most literature values although the magnitude of ϵ for HONO varies in these studies as summarized in Table 4. Good agreement with the gas-phase value (for the second vibronic band) of HONO is found for the results of the current study. A small but expected shift in the vibronic bands is observed: the actual absorbance maximum in the gas-phase being measured at 368 nm (ϵ_{max} 116.5 M^{-1} cm^{-1}). Although this figure is larger than all solution values reported, it is of the same magnitude.[7] The solution spectra are therefore clearly similar to the gas-phase counterpart. However it should be noted that the spectra obtained by both Arakaki et al. and Fischer and Warneck[34] were obtained from highly acidified nitrite ion solutions and, therefore, subject to the possible source of quantitation error mentioned above.

The molar absorption coefficient of total N(III) at a pH value ($\epsilon_{N(III),\lambda}$) can be determined from the ϵ values for both NO_2^- and HONO, using the following formula:

$$\epsilon_{N(III),\lambda} = f_{HNO_2}\epsilon_{HNO_2,\lambda} + f_{NO_2^-}\epsilon_{NO_2^-,\lambda} \qquad (17)$$

where f_{HNO_2} and $f_{NO_2^-}$ are the fractions of HNO_2 and NO_2^- at a certain pH and $\epsilon_{HNO_2,\lambda}$ and $\epsilon_{NO_2^-,\lambda}$ are the molar absorption coefficients at a wavelength, λ.

The pK_a of HONO is most often quoted as 3.27,[11] but values in the literature ranging from 2.3 to 5.22 [35] have been reported. Therefore, the pK_a was reevaluated from the new set of data obtained in this work.

TABLE 3: N(III) Molar Absorption Coefficient Data

λ/nm	$\epsilon_{NO_2^-},\lambda$	ϵ_{HNO_2},λ	λ/nm	$\epsilon_{NO_2^-},\lambda$	ϵ_{HNO_2},λ	λ/nm	$\epsilon_{NO_2^-},\lambda$	ϵ_{HNO_2},λ
270	6.46	2.98	314	9.30	5.19	358	21.66	57.05
271	6.59	2.55	315	9.43	5.76	359	21.60	56.47
272	6.70	2.15	316	9.59	6.34	360	21.49	53.79
273	6.83	1.81	317	9.75	6.86	361	21.19	49.68
274	6.94	1.51	318	9.92	7.35	362	20.98	45.51
275	7.05	1.24	319	10.12	7.83	363	20.55	42.38
276	7.16	1.00	320	10.33	8.37	364	20.10	40.95
277	7.26	0.81	321	10.55	9.04	365	19.82	41.28
278	7.35	0.64	322	10.79	9.90	366	19.23	43.20
279	7.45	0.50	323	11.06	10.92	367	18.86	46.28
280	7.54	0.37	324	11.36	11.98	368	18.19	50.20
281	7.62	0.28	325	11.65	12.95	369	17.43	54.47
282	7.70	0.19	326	11.96	13.70	370	16.88	58.23
283	7.77	0.12	327	12.28	14.26	371	16.18	60.46
284	7.83	0.07	328	12.63	14.76	372	15.48	60.52
285	7.89	0.03	329	13.00	15.37	373	14.79	57.82
286	7.95	0.00	330	13.39	16.28	374	14.02	52.40
287	7.99	0.00	331	13.75	17.53	375	13.23	45.78
288	8.04	0.00	332	14.15	19.21	376	12.47	39.39
289	8.08	0.00	333	14.56	21.12	377	11.85	34.18
290	8.13	0.02	334	15.00	22.94	378	11.04	30.69
291	8.16	0.06	335	15.42	24.34	379	10.35	28.87
292	8.18	0.10	336	15.91	25.07	380	9.61	28.42
293	8.21	0.16	337	16.34	25.25	381	8.92	29.09
294	8.22	0.24	338	16.81	25.20	382	8.18	30.50
295	8.27	0.31	339	17.23	25.42	383	7.51	32.28
296	8.29	0.40	340	17.72	26.25	384	6.86	34.18
297	8.29	0.51	341	18.18	27.82	385	6.23	35.74
298	8.33	0.64	342	18.61	30.19	386	5.61	36.53
299	8.36	0.78	343	19.04	33.20	387	5.02	36.09
300	8.35	0.96	344	19.47	36.35	388	4.51	34.06
301	8.40	1.12	345	19.89	39.08	389	4.03	30.59
302	8.43	1.31	346	20.14	40.70	390	3.53	25.99
303	8.46	1.50	347	20.65	40.76	391	3.04	20.87
304	8.50	1.69	348	20.90	39.58	392	2.64	16.06
305	8.56	1.95	349	21.09	37.93	393	2.29	11.97
306	8.61	2.23	350	21.41	36.67	394	2.01	8.86
307	8.66	2.53	351	21.59	36.49	395	1.68	6.39
308	8.72	2.86	352	21.86	37.59	396	1.38	4.66
309	8.82	3.17	353	21.96	40.06	397	1.11	3.38
310	8.89	3.48	354	21.97	43.67	398	0.91	2.50
311	8.97	3.81	355	22.10	48.02	399	0.77	1.87
312	9.08	4.20	356	22.02	52.26	400	0.61	1.44
313	9.18	4.67	357	21.95	55.53			

TABLE 4: Comparison of ϵ Values for the Second Vibronic Band of Aqueous HONO

ϵ/M^{-1} cm-1	ref
51.90 ± 0.50	Arakaki et al.[13]
74.14	Graedel and Weschler[39]
43.25	Fischer and Warneck[34]
60.52 ± 0.60	current study

TABLE 5: Comparative Summary of the pK_a Values for HONO

	pK_a using HCl		pK_a using H_2SO_4	
$[NO_2^-]$/mol L^{-1}	method 1	method 2	method 1	method 2
0.02	3.1	2.9	2.8	2.9
0.03	3.2	2.5	3.0	2.8
0.04	3.2	2.8	3.0	2.8
0.06	3.2	2.4	3.1	2.9
average	3.2 ± 0.1	2.7 ± 0.2	3.0 ± 0.1	2.8 ± 0.1

Determination of the pK_a Value for Nitrous Acid. The spectroscopic determination of the pK_a of weak acids described by Albert and Serjeant is applied here.[36] This method (termed method 1 in Table 5) involves the measurement of the individual spectra of pure acidic solutions of HONO and the pure ionic, NO_2^-, species. The so-called "analytical wavelength", i.e., the wavelength at which the two spectra show the greatest absorbance difference, is used in the following formula to evaluate pK_a:

$$\mathrm{pK_a} = \mathrm{pH} + \log\frac{A_I - A}{A - A_M} \tag{18}$$

where A_I, A_M, and A are the absorbance values at the analytical wavelength of the spectrum for the pure ionic species, the pure molecular species, and the sample solution respectively.

Although this relationship is merely a rearrangement of the Henderson−Hasselbalch equation, it is subject to the same problems of HONO concentration overestimation discussed above. Hence an alternate method of spectral analysis was applied (termed method 2 in Table 5). In this approach, the more rigorous baseline subtraction approach described in the previous section was used to evaluate the concentrations of nitrite ion and nitrous acid in solution at each pH.

A more conventional formulation of the Henderson−Hasselbalch eq 19 is then used to calculate the pK_a value. For this method, only spectra in the pH range 6−3 are required

$$\mathrm{pH} = \mathrm{pK_a} + \log\frac{[\mathrm{A^-}]}{[\mathrm{HA}]} \tag{19}$$

where A^- refers to the ionic species, NO_2^-, and HA to the molecular acid, HONO.

The principal source of error in the experiment was encountered in the measurement of H^+ concentration. The pH meter employed reports values to ±0.1 of a pH unit. Since the errors associated with the spectroscopic absorbance measurements are very small in comparison, the calculated pK_a values are assumed to contain an error of ±0.1.

The results obtained from the two methods are summarized in Table 5. Independent experiments using HCl and H_2SO_4 for acidification of the nitrite ion are included but show no significant difference. The first point of note regarding the results is that there is no variation of pK_a value as a function of nitrite ion concentration. The use of concentration data in studies of this type is, of course, acceptable only in the case of appropriately dilute solutions. Generally when the amounts of species in solution are increased, concentrations must be corrected with appropriate activity coefficients. However as the concentrations utilized in this study lead to reproducible pK_a values, the omission of activity coefficients would appear to be justified. This point is further elaborated upon in the following discussion of the numerical modeling of the system.

A second point to be noted is that the pK_a values determined using the Albert method (method 1) are consistently higher than those from the method developed in this study (method 2). It is obvious from the Henderson−Hasselbalch equation (equation 18) that the pK_a is dependent on the numerical value of the quotient, $[NO_2^-]$/[HONO]. Overestimations of the HONO concentration will decrease this quotient and increase the calculated value for the pK_a. Thus the lower values obtained using method 2 are probably a more accurate determination of the dissociation constant from the spectra. Hence, a value of 2.8 ± 0.1 is reported here for the dissociation constant of nitrous acid.

As mentioned earlier, the published literature contains values for the pK_a of HONO which range from 2.30 to 5.22. The only previous spectroscopic pK_a determination appears to have been performed by Gomes and Borges.[35] Using the Albert and Serjent treatment, they reported a value of 2.2, which represents the lowest published value. The other data originate from earlier

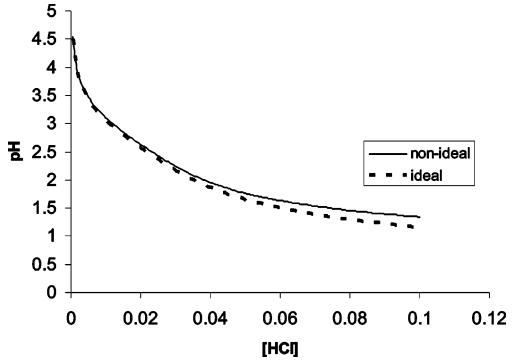

Figure 3. Modeling graph of pH vs [HCl] addition for ideal ($\gamma_{\pm} = 1$) and nonideal ($\gamma_{\pm}$ from Pitzer equation) systems (0.03 M nitrite ion concentration).

potentiometric and conductivity experiments. Although the value obtained in the current study (2.8) is outside the error limit of Gomes and Borges, the two spectroscopic determinations are similar enough to call into question the commonly quoted literature values of 3.2−3.3.[13]

Numerical Modeling Studies: The One Step Equilibrium Process. The initially modeled system consisted of four variables: [HONO], [NO_2^-], [H^+] and [OH^-]. Four equations were solved in the model to evaluate these quantities using the experimentally determined nitrous acid dissociation constant (K_a) and the ionic product of water (K_w) as the limiting parameters.

To keep the model free from unnecessary complication, it was written to account for the addition of a strong monoprotic acid to the N(III) solution. Clearly, at a highly acidic pH, the formation of bisulfate ions (HSO_4^-) may be expected to occur (pK_a $HSO_4^- = 1.92$) when sulfuric acid is used as the H^+ source. For the model to function accurately, two additional variables (sulfate and bisulfate ions) and two new equations (the sulfate mass balance and the dissociation of bisulfate ion) would need to be included. Therefore, the devised program is best applied to the acidic condition when HCl is added to the nitrite ion solutions (pK_a for HCl = −6.23 [37]) and the results discussed below refer to this system. It should be pointed out that the *experimentally* determined values of pK_a obtained in this study when H_2SO_4 is used as the H^+ source are not devalued because the calculations depend only upon pH and N(III) concentrations, and not on the quantities of acid in solution. Finally in the relatively highly concentrated solutions under investigation in this study, any escape of HONO from the liquid to the gas-phase will have a negligible effect on bulk concentrations (due to its Henry's law constant). Therefore, this step has not been included in the model.

The numerical model was then used to demonstrate the effect (or otherwise) of activity coefficients on the system. In the Experimental Section, it was concluded that changes in the magnitude of $\gamma_{\pm}$ with nitrite ion concentration did not alter the outcome of the calculations for the current experimental determination of the pK_a significantly. This can be confirmed by inspection of the numerical model output because, by use of the Pitzer equation, it can be used to calculate the activities of the species in solution. Alternatively, it can be configured to ignore activity coefficients and treat the system as ideal. For example, with the addition of HCl to a 0.03 M $NaNO_3$ solution using the experimentally determined value of 2.8 for the dissociation constant it is found that as the pH decreases below 4, the variation from ideality becomes apparent but remains small. Even at its maximum, the difference between the systems is less than 0.2 of a pH unit as shown in Figure 3. A deviation

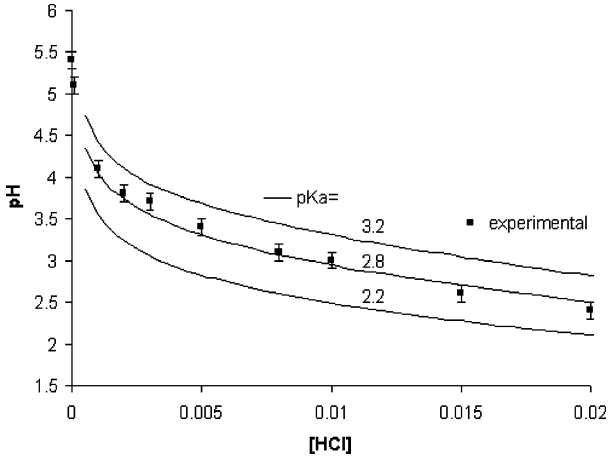

Figure 4. pH vs [HCl] modeling graph for a 0.03M $NaNO_2$ solution using a range of pK_a values to compare with current experimental study.

of this magnitude is similar to the experimental error, and therefore, it is not surprising that the omission of activity coefficients does not affect the reproducibility of the measured results. To further illustrate this point, it was determined that with much more highly concentrated $NaNO_2$ solution (0.1 M) than used in the experiments, the deviation from ideality becomes considerably more pronounced: here the difference between the two systems exceeded 0.5 of a pH unit in some regions of the profile.

The most useful feature of the model is its application to the verification of the experimentally measured pK_a value. Again, simply by altering the pK_a value line of code in the program, the response of pH to acid added can be investigated using a range of acid dissociation constants. Figure 4 shows the model output for three different pK_a values utilizing a 0.03 M $NaNO_2$ solution along with the experimental results obtained in the current study shown for comparison. For this concentration, the pK_a value of 2.8 fits the experimental values well in the pH region 6−3. The pK_a value of 2.2 (as determined by Gomes and Borges) is not a good fit for the model and underestimates the pH over the entire range. The commonly quoted literature value of 3.27 on the other hand consistently predicts a higher pH than is observed in this study. Although this comparison does not provide independent verification of the experimental values reported in this study, it does show that the calculated value of 2.8 is a better fit than any value above 3. Therefore, the treatment of spectral data devised in this study (method 2) would appear to more accurately determine the acid dissociation constant than the Albert and Serjent[36] approach (method 1), which is used most often in the literature.

Simple modeling graphs of pH vs [HCl] are not the only output that the program provides. The model can also be configured to display how the equilibrium concentrations of the species in solution vary with pH. A plot of HONO mole fraction vs pH represents the most efficient way to average all of the experimental runs because the total N(III) concentration is not then a factor. It is apparent in Figure 5 that the model works quite well for intermediate pHs (6−3) but departs from the experimental observations in highly acidic media. Possible reasons for this divergence are discussed below.

Numerical Modeling Studies: Two-Step Equilibrium Processes. As discussed above the behavior of nitrous acid under highly acidic condition has been explored both experimentally and theoretically by a diversity of researchers. Using a numerical modeling approach, the plausibility of a second protonation step,

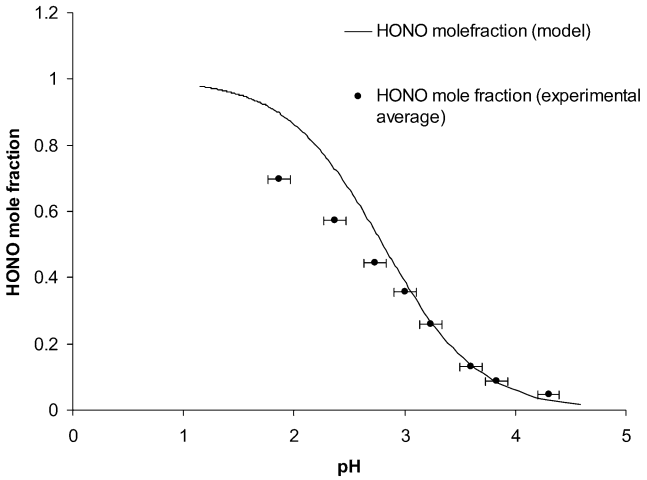

Figure 5. Mole fraction of HONO vs pH comparison for model and experimental results.

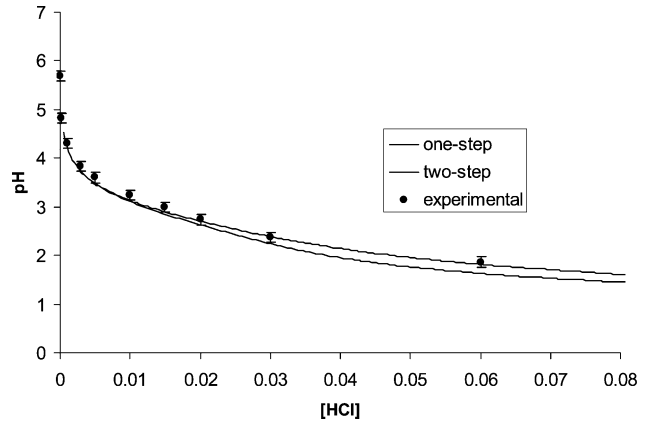

Figure 6. Model comparisons between one-step and two-step systems for HONO.

as in reaction 20, can be examined and then compared with the available experimental measurements

$$\mathrm{HONO} + \mathrm{H_3O^+} \rightleftharpoons \mathrm{H_2ONO^+} + \mathrm{H_2O} \qquad (20)$$

Overall the underlying chemistry is best summarized by the two-step reaction shown as reaction 5

$$\mathrm{NO_2^-} \overset{\mathrm{H^+}}{\rightleftharpoons} \mathrm{HONO} \overset{\mathrm{H^+}}{\rightleftharpoons} \mathrm{H_2ONO^+} \qquad (21)$$

Figure 6 is a plot of pH vs HCl addition for a 0.03 M nitrite ion system. Clearly, the one-step model (using the experimentally determined pK_a of 2.8) mimics the experimental values closely in the intermediate pH region (6−3). However, as acidity increases toward pH ≈ 2.7, there is a clear drift in the simulated values outside the error range of the laboratory results. In this region, pH appears not to decrease as rapidly as acid is added. The two-step model is a much closer fit in the very acidic region, while having little or no effect on the intermediate section of the profile. The dissociation constant used for the second step (pK_{a1}) was 1.5. This number has no physical significance and was chosen merely as the value that fits the experimental results most closely. In any case, the two-step equilibrium model does fit the experimental results better than the commonly accepted one-step process at very low pH.

Finally the model was re-configured to display equilibrium speciation in the system (Figure 7). No appreciable amount of the nitroacidium ion appears to exist until the level of acidity

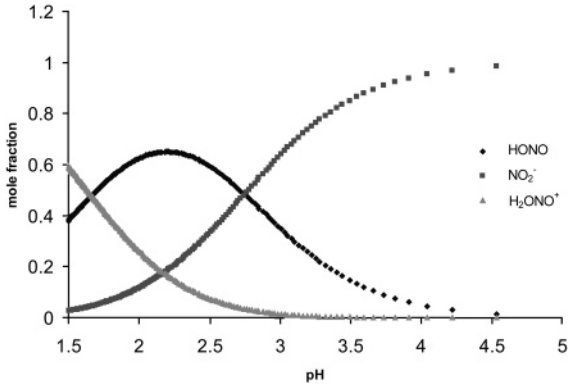

Figure 7. Model simulation of speciation for the two-step equilibrium process.

reaches pH ≈ 2.4. As the pH decreases further, the fraction of H_2ONO^+ increases until at pH ≈ 1.5, it becomes the principal species in solution.

Conclusion

The spectra of the N(III) compounds, nitrite ion (NO_2^-) and nitrous acid (HONO) were recorded from 200 to 400 nm. The addition of mineral acid to the N(III) solutions to lower the pH was found to increase the mole fraction of HONO at the expense of NO_2^-. Using the change in speciation with respect to pH and a careful spectral subtraction procedure, the acid dissociation constant (K_a) of nitrous acid was evaluated as 1.6×10^{-3} mol dm^{-3} (p$K_a = 2.8 \pm 0.1$), which is somewhat lower than the currently accepted literature value. The spectra also allowed determination of the molar absorption coefficients of the two species in the UV−vis region. Nitrite ions were shown to display a maximum absorbance at 354 nm ($\epsilon = 22.1 \pm 0.22$ M^{-1} cm^{-1}), whereas that of nitrous acid occurs at 372 nm ($\epsilon = 60.5 \pm 0.60$ M^{-1} cm^{-1}). The above findings may have important bearings on hydroxyl radical solution chemistry and photochemistry

Numerical modeling was used to investigate the possible protonation of HONO at pH values below 3 to form the nitrous acidium ion (H_2ONO^+), a species which is generally not included in atmospheric models. Two equilibria did indeed fit the full data better than a one-step process. Hence the acid dissociation constant for the doubly protonated ion was calculated to be 2×10^{-2} mol dm^{-3} (p$K_a = 1.7$). Its potential participation in highly acidic atmospheric waters may initiate reactions with halide ions.

Acknowledgment. We thank Dr. Justin Holmes and Dr. Kirk Ziegler for their comprehensive introduction to us of the techniques associated with optimization modeling.

References and Notes

(1) Vione, D.; Maurino, V.; Minero, C.; Pelizzetti, E. *Chemosphere* **2001**, *45*, 893−902.
(2) Zuo, Y. G.; Deng, Y. W. *Chemosphere* **1998**, *36*, 181−188.
(3) Cape, J. N.; Hargreaves, K. J.; Storetonwest, R.; Fowler, D.; Colvile, R. N.; Choularton, T. W.; Gallagher, M. W. *Atmos. Environ. Part a-Gen. Top.* **1992**, *26*, 2301−2307.
(4) Sharp, J. H. *Nitrogen Marine Environ.* **1983**, 1−35.
(5) Bambauer, A.; Brantner, B.; Paige, M.; Novakov, T. *Atmos. Environ.* **1994**, *28*, 3225−3232.
(6) Seinfeld, J. H.; Pandis, S. N. *Atmospheric Chemistry and Physics*; Wiley-Interscience: New York, 1997.
(7) Finlayson-Pitts, B. J.; Pitts, J. N., Jr. *Chemistry of the Upper and Lower Atmosphere*; Academic Press.: New York, 2000.
(8) Zafiriou, O. C.; True, M. B. *Marine Chem.* **1979**, *8*, 9−32.
(9) Zellner, R.; Exner, M.; Herrmann, H. *J. Atmos. Chem.* **1990**, *10*, 411−425.

(10) Anastasio, C.; McGregor, K. G. *Atmos. Environ.* **2000**, *35*, 1079−1089.
(11) Arakaki, T.; Miyake, T.; Shibata, M.; Sakugawa, H. *Nippon Kagaku Kaishi* **1998**, 619−625.
(12) Arakaki, T.; Faust, B. C. *J. Geophys. Res.-Atmos.* **1998**, *103*, 3487−3504.
(13) Arakaki, T.; Miyake, T.; Hirakawa, T.; Sakugawa, H. *Environ. Sci. Technol.* **1999**, *33*, 2561−2565.
(14) Li, S. M.; Macdonald, A. M.; Strapp, J. W.; Lee, Y. N.; Zhou, X. L. *J. Geophys. Res.-Atmos.* **1997**, *102*, 21341−21353.
(15) Longfellow, C. A.; Imamura, T.; Ravishankara, A. R.; Hanson, D. R. *J. Phys. Chem. A* **1998**, *102*, 3323−3332.
(16) Nguyen, M.-T.; Hegarty, A. F. *J. Chem. Soc., Perkin Trans. 2* **1984**, 2037−2041.
(17) Allan, G. G.; Peyron, M. *Carbohydr. Res.* **1995**, *277*, 257−272.
(18) Grossi, L.; Montevecchi, P. C. *J. Org. Chem.* **2002**, *67*, 8625−8630.
(19) Pestovsky, O.; Bakac, A. *Inorg. Chem.* **2002**, *41*, 901−905.
(20) Dargelos, A.; Elouadi, S.; Liotard, D.; Chaillet, M.; Elguero, J. *Chem. Phys. Lett.* **1977**, *51*, 545−551.
(21) Edwards, W. D.; Weinstein, H. *Chem. Phys. let.* **1978**, *56*, 582.
(22) Francisco, J. S. *J. Chem. Phys.* **2001**, *115*, 2117−2122.
(23) Atkins, P. *Physical Chemistry*, 5th ed.; Oxford University Press: New York, 1994.
(24) Strickler, S.; Kasha, M. *J. Am. Chem. Soc.* **1963**, *85*, 2899.
(25) Trawick, W. G.; Eberhardt, W. H. *J. Chem. Phys.* **1954**, *22*, 1462.
(26) Mulliken, R. *Rev. Mod. Phys.* **1942**, *14*, 204−215.
(27) Walsh, A. *J. Chem. Soc.* **1953**, 2266−89.
(28) Sidman, J. *J. Am. Chem. Soc.* **1957**, *79*, 2669.
(29) Schwartz, S. E.; White, W. H. *Adv. Environ. Sci. Eng>* **1981**, *4*, 1−45.
(30) Brust, A. S.; Becker, K. H.; Kleffmann, J.; Wiesen, P. *Atmos. Environ.* **2000**, *34*, 13−19.
(31) Nakamoto, K. *Infrared and Raman Spectra of Inorganic and Coordination Compounds*; John Wiley and Sons Inc.: New York, 1997; Vol. 2.
(32) NIST. Standard Reference Database; NIST: Gathersburg, MD, 2003.
(33) Pagsberg, P.; Bjergbakke, E.; Ratajczak, E.; Sillesen, A. *Chem. Phys. Lett.* **1997**, *272*, 383−390.
(34) Fischer, M.; Warneck, P. *J. Phys. Chem.* **1996**, *100*, 18749−18756.
(35) Gomes, M.; Borges, S.; Lopes, L.; Franco, D. *Anal. Chim. Acta* **1993**, *282*, 81−85.
(36) Albert, A.; Serjeant, P. E. *The Determination of Ionization Constants*, 2nd ed.; Chapman and Hall, Edinburgh, U.K., 1971.
(37) Harris, D. *Quantitative chemical analysis*, 3rd ed.; Freeman: New York, 1991.
(38) Wetters, J.; Uglum, K. *Anal. Chem.* **1970**, *42*, 313.
(39) Graedel, T. E.; Weschler, C. J. *Rev. Geophys.* **1981**, *19*, 505−539.